doi:10.1016/j.jmb.2007.08.054 J. Mol. Biol. (2007) 373, 1058–1070

JMB

Available online at www.sciencedirect.com
ScienceDirect

ELSEVIER

Analysis of Structural Dynamics in the Ribosome by TLS Crystallographic Refinement

Andrei Korostelev and Harry F. Noller*

Center for Molecular Biology of RNA and Department of Molecular, Cell and Developmental Biology University of California at Santa Cruz, Santa Cruz CA 95064, USA

Received 27 May 2007; received in revised form 13 July 2007; accepted 23 August 2007
Available online
29 August 2007

A major goal in the study of ribosome structure and function is to obtain a complete description of the conformational dynamics of the ribosome during the many steps of protein synthesis. Here, we report a new approach to the study of ribosome dynamics using translation-libration-screw (TLS) refinement against experimental X-ray diffraction data. TLS analysis of complexes of the 70 S ribosome suggests that many of its structural features have an inherent tendency for anisotropic movement. Analysis of displacements of the 30 S and 50 S ribosomal subunits reveals an intrinsic bias for "ratchet-like" intersubunit rotation. The libration axes for both subunits pass through the peptidyl transferase center (PTC), indicating a tendency for structural rotations to occur around the site of peptide bond formation. The modes of anisotropic movement of ribosomal RNA components, including the head of the 30 S subunit, the L1 and L11 stalks and the two main arms of the tRNAs were found to correlate with their respective modes of movement previously inferred from comparisons of ribosomes trapped in different functional states. In the small subunit, the mobilities of features interacting with the Shine–Dalgarno helix are decreased in the presence of the Shine–Dalgarno helix, supporting the proposal that that formation of the Shine–Dalgarno helix during initiation may contribute to stabilization of the small subunit for optimal interaction with initiator $tRNA^{fMet}$. The similarity of TLS parameters for two independently solved structures of similar ribosome complexes suggests that TLS analysis can provide useful information about the dynamics of very large macromolecular objects and at resolutions lower than those at which TLS refinement has commonly been applied.

Keywords: structural dynamics; 70 S ribosome; TLS refinement; X-ray crystallography

Edited by J. Doudna

Introduction

Ribosomes are the ribonucleoprotein particles responsible for converting genetic information encoded in messenger RNA (mRNA) into proteins. During protein synthesis, transfer RNAs (tRNAs) deliver amino acids to the ribosome. Recognition of the cognate aminoacyl-tRNA for each mRNA codon (decoding process) occurs on the small (30 S) subunit and is followed by peptide bond formation in the peptidyl-transferase center (PTC) of the large subunit. Each cycle of elongation is followed by translocation of tRNAs through the ribosome, during which tRNA moves from the A (aminoacyl) site to the P (peptidyl) site and then to the E (exit) site before leaving the ribosome. These functional processes are accompanied by rapid, large-scale molecular movements of tRNA, mRNA and translation factors that are believed to be accompanied by corresponding movements in the structure of the ribosome. For example, comparison of cryo-electron microscopic reconstructions of ribosomes trapped in different states of translocation has led to a model for translocation based on intersubunit rotation[1] that has recently been supported by solution studies

*Corresponding author. E-mail address: rna@biology.ucsc.edu.

Abbreviations used: TLS, translation-libration-screw; PTC, peptidyl transferase center; cryo-EM, cryo-electron microscopy; SD, Shine–Dalgarno.

using FRET[2] and intersubunit cross-linking.[3] Although translocation normally requires participation of elongation factor EF-G and GTP, it has been shown to occur in their absence under certain *in vitro* conditions,[4–8] indicating that the ribosome has an inherent ability to undergo the conformational rearrangements required for translocation. It seems likely that the structure of the ribosome has been optimized during evolution to support these and other dynamic events that underlie protein synthesis. A major goal in the study of ribosome structure and function is to obtain a full description of the molecular dynamics of translation, in terms of the structures of the ribosome and its functional ligands. The studies presented here suggest a novel approach toward this end.

Since the magnitudes and directionalities of atomic displacements are captured in diffraction data,[9] these data can be exploited to infer information about macromolecular dynamics. Attributing individual atomic anisotropic displacement parameters to a model, however, is possible only when high-resolution (better than 1.2 Å) diffraction data are available.[10] However, at lower resolutions (commonly 1.2 to 3 Å),[11] translation-libration-screw (TLS) formalism can be applied to rigid domains, rather than to individual atoms, and has been demonstrated to closely approximate the anisotropic behavior of an atomic model.[12,13] Comparison of TLS parameters with the amplitudes of normal modes describing the internal motion of a protein indicates that TLS parameters for the overall motion make the largest contribution to atomic displacements.[14,15] TLS analysis has been shown to provide biologically relevant information, such as identification of mobile domains contributing to induced fit of a protein as well as of regions of restricted mobility, comprised of biologically critical sites, such as the active sites of enzymes.[16,17] The theory underlying TLS parameterization has been presented in detail by Schomaker and Trueblood[18,19] and Howlin *et al.*[20] In summary, apart from improving agreement between an atomic structure and diffraction data by approximating anisotropic disorder of atoms, TLS refinement yields translational, librational and screw tensors for the respective rigid groups. The collective anisotropic disorder of atoms representing each rigid group can therefore be described as translation along translational axes, torsional oscillations around librational axes and screw motions along screw axes. In this work, TLS formalism has allowed visualization of the anisotropic dynamics of the ribosomal subunits and their sub-structures, and tRNAs bound to the ribosome.

Results

TLS refinement

The structure used for TLS analysis represents an elongation-like ribosomal complex containing a short ten-nucleotide defined mRNA, $tRNA^{Phe}$ bound to the P site and an endogenous mixture of tRNAs bound to the E site (modeled as $tRNA^{Phe}$), determined at 3.7 Å resolution,[21] referred to below as the $tRNA^{Phe}$ complex. TLS refinement followed a conventional refinement strategy and led to reduction in crystallographic *R* and free *R* factors, indicating improvement of the fit of the structural model to the experimental diffraction data. Comparison of the relative magnitudes of translational, librational and screw tensor eigenvalues showed that TLS motion is primarily characterized by libration (see Materials and Methods). The focus of the following discussion will therefore be on the libration axes obtained by treating the $tRNA^{Phe}$ complex as either 4 or 70 independent TLS groups, as well as on comparison of librational movements with those of the crystal structure of a separate ribosome–tRNA complex recently solved at similar resolution.[22]

TLS parameterization of the ribosome represented by four rigid groups

Cryo-EM, biochemical and biophysical studies suggest that movement of ribosomal subunits during translocation can be approximated as a ratchet-like intersubunit rotation.[1–3] In order to explore the inherent tendency of the subunits to move, TLS refinement was performed with the 30 S subunit, 50 S subunit and P and E-site tRNAs treated as four separate TLS groups. For each subunit, the librational components are anisotropic (the magnitudes of the primary axes are 2.5-and fivefold higher than that of the second largest axis for the large and small subunit, respectively) and imply that inherent intersubunit movement is biased towards ratchet-like libration (Figure 1(a)–(c)). For the large subunit, the primary librational axis, around which the subunit as a rigid group undergoes the largest anisotropic displacement, nearly coincides with that of the small subunit (Figure 1(a) and (b)). This main axis of the large subunit connects the peptidyl transferase center with proteins L20 and L21 on the solvent side of the subunit. The primary axis of the small subunit penetrates the subunit through the penultimate stem (h44) between nucleotides U1407 and A1492–A1493 in the decoding site[23] and through the cleft formed by proteins S2, S5 and S8 at the solvent side. Thus, the major librational axes for the two ribosomal subunits pass through their respective main functional sites. Interestingly, for both subunits, the libration axes intersect near the peptidyl-transferase center (PTC). One possible explanation is that the inherent ribosomal mobility is tuned to minimize disruption of the conformation of the PTC during different steps of protein synthesis, to ensure precise aligment of the ribosomal nucleotides forming the PTC during catalysis. This might be important, for example, to exclude attack by water of the peptidyl–tRNA linkage.[24] Another possibility is that the structure of the ribosome is optimized for rotation of the aminoacyl–

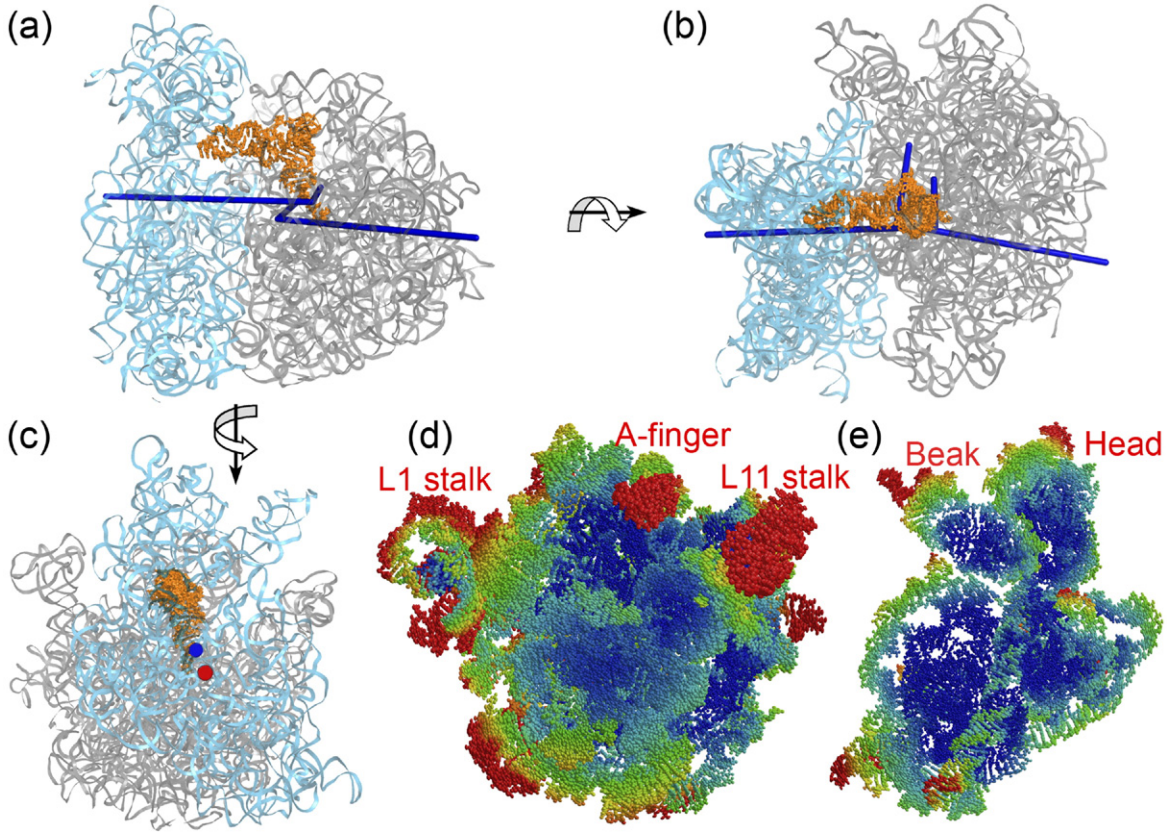

Figure 1. Libration axes and thermal ellipsoids for the 30 S and 50 S ribosomal subunits. P-site tRNA (orange), 16 S (cyan) and 23 S (grey) rRNAs, and libration axes derived from a 4-TLS group refinement (blue) are shown. (a) Side view, (b) top view, (c) view from the solvent face of the 30 S subunit showing the location of the principal libration axis derived from the 4-TLS group refinement (blue) and of the intersubunit ratcheting axis suggested by cryo-EM experiments[28] (red). (d) and (e) Thermal ellipsoids derived from the 70 S-TLS group refinement for the large and small ribosomal rRNAs viewed from the subunit interface. Atomic displacement parameters in this and the following figures are colored according to the magnitude of the displacements, ramped from blue (smallest) to red (largest). The directional anisotropy of peripheral regions and the lack of mobility in the central regions suggest an inherent bias for rotation of the ribosomal subunits in a "ratchet-like" mode.

and peptidyl–tRNAs around the PTC during their movements before, during and following catalysis. It should also be taken into account that the PTC is located near the center of the ribosome, and is therefore less likely to show large displacements of the kind that are observed at the extremities of the ribosome.

The orientations and magnitudes of libration axes for the P and E-site tRNAs show a striking correlation with the distortions of the tRNAs caused by their interactions with the ribosome.[21,25] The two longest librational axes of the E-site tRNA are nearly equal in magnitude (Figure 2(a)). Rotation of the structure of free tRNA by 4° and 7° consecutively around the E-tRNA libration reproduces the kink observed in the E-tRNA structure relative to that of free tRNA,[21] suggesting that the libration axes reflect the inherent directionality of E-tRNA movements. The librational motion of P-tRNA is highly anisotropic, and the relative eigenvalues of its libration tensor are greater than those for the E-tRNA (Figure 3(a)), consistent with the higher degree of distortion of the P-tRNA observed in the X-ray crystal structures.[21,25] Its primary axis goes through the D loop and between the A26–G44 non-canonical base-pair, making a ~45° angle with the anticodon stem–loop of P-tRNA; its second libration axis is orthogonal to the helical axis of the D stem. Interestingly, rotation of tRNA by ~10° around the primary axis followed by ~5° rotation around the second axis generates the kink in the anticodon arm centered at the A26–G44 pair which has been observed in the P, E and A/T states of tRNA.[21,25,26] However, the observed distortion of the D loop, which is partially unwound only in the P-tRNA, orienting the acceptor arm towards the A site, cannot be generated by rotation around libration axes; this distortion would require rotation around the third libration axis, whose magnitude is 0. This may be an indication that treating tRNA as a single rigid group may be insufficient to account for the complexity of the distortion of tRNA conformation in the P site.

The center of libration for both P and E-site tRNAs is located near the D stem (Figures 2(a) and 3(a)), which leads to roughly similar distributions of the relative anisotropic disorder of the atoms. Representation of the TLS parameters in terms of atomic

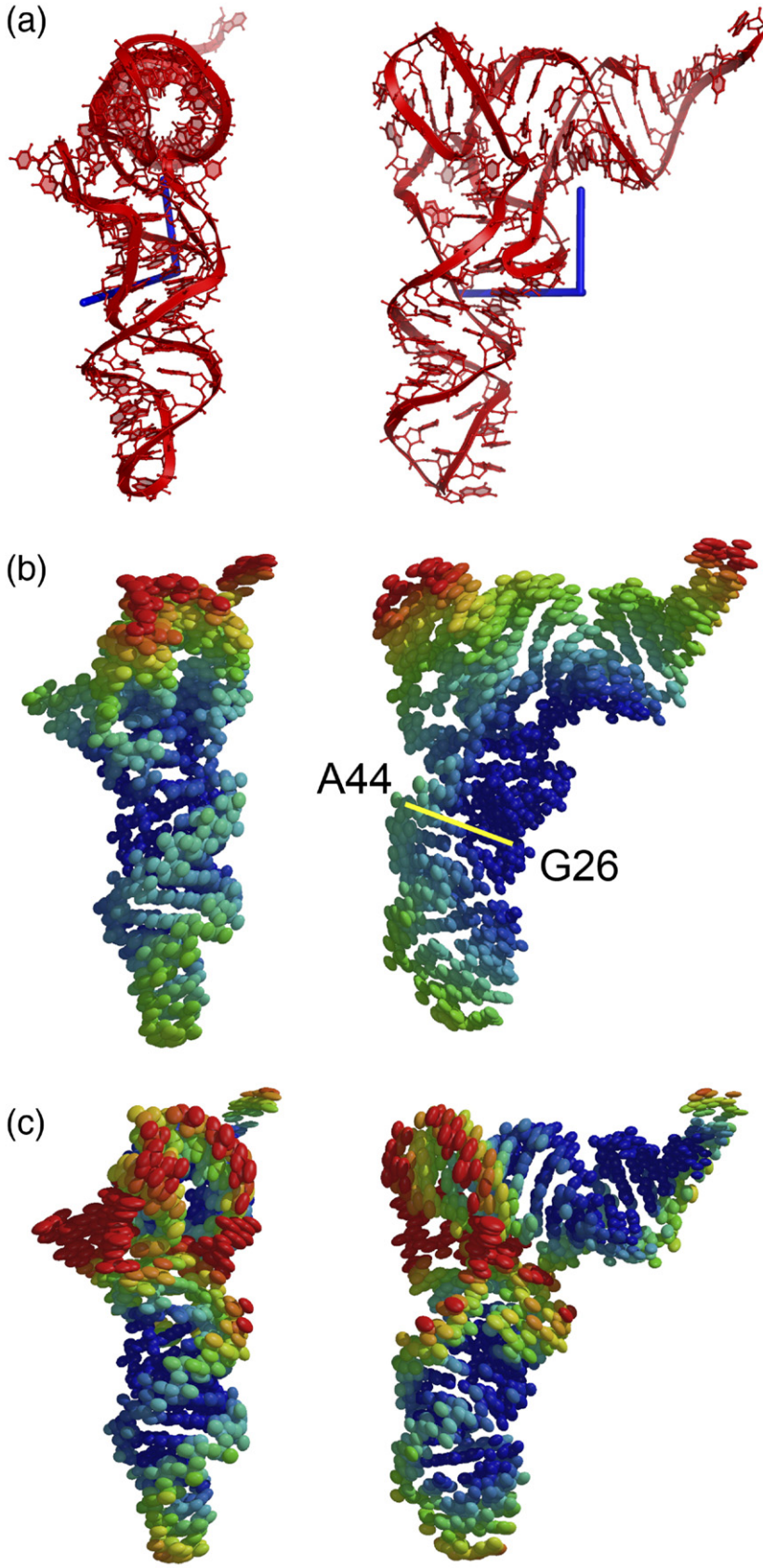

Figure 2. Libration axes and thermal ellipsoids for the E-site tRNA. (a) Libration axes. (b) Thermal ellipsoids for E-site tRNA represented as a single TLS group in a 4-TLS group refinement of the ribosome. (c) Thermal ellipsoids for E-site tRNA represented as 2 TLS groups in a 70-TLS group refinement of the ribosome.

anisotropic displacement parameters suggests that in the P and E-site tRNAs the A26–G44 base-pair is among the least mobile regions (Figures 2(b) and 3(b)), consistent with the conclusion that this base-pair represents one of the main hinge points of tRNA distortion.[21,26] The most mobile region of

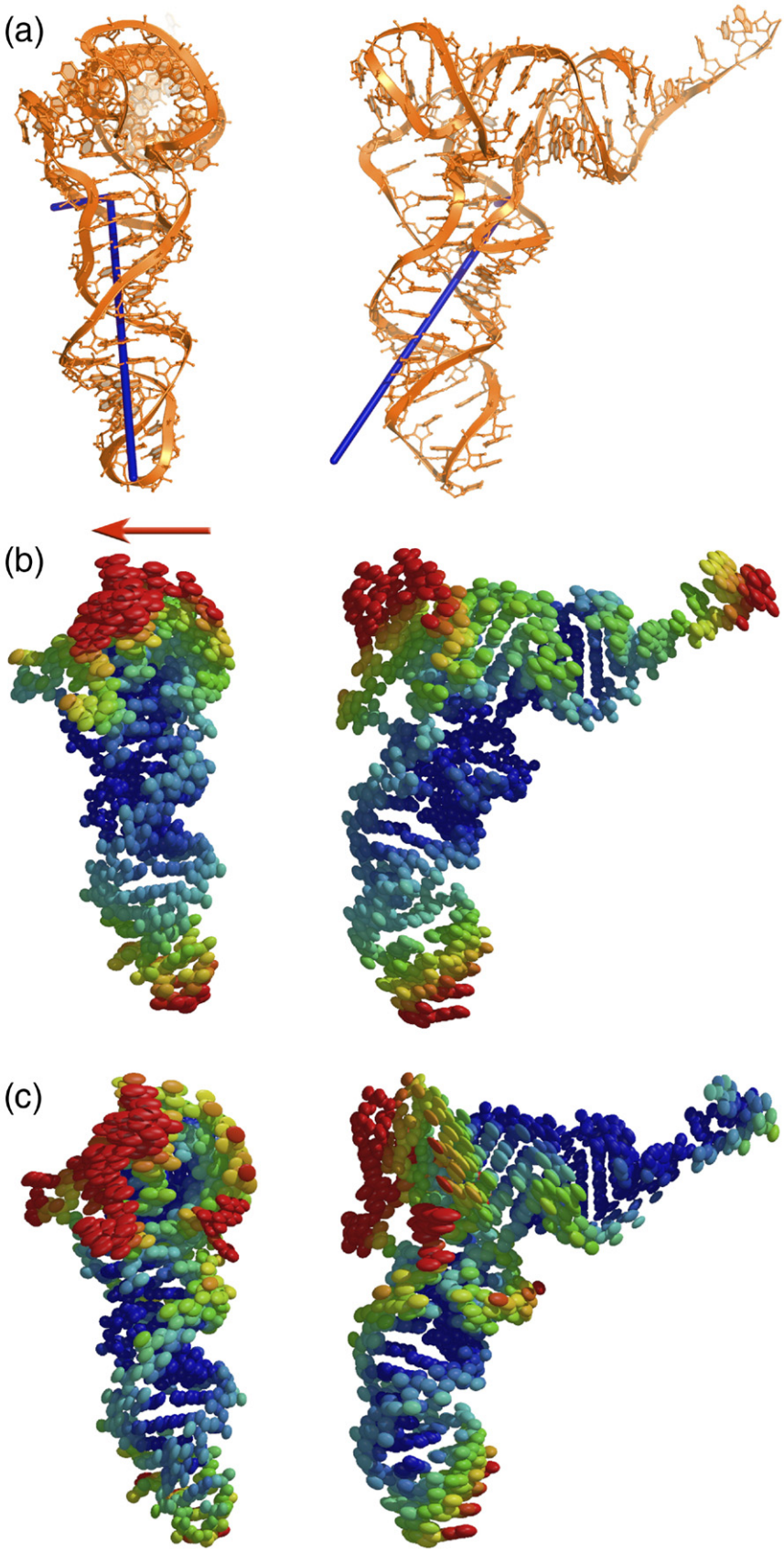

Figure 3. Libration axes and thermal ellipsoids for the P-site tRNA. (a) Libration axes. (b) Thermal ellipsoids for P-site tRNA represented as a single TLS group in a 4-TLS group refinement of the ribosome. Direction of translocation is shown by a red arrow. (c) Thermal ellipsoids for P-site tRNA represented as two TLS groups in a 70-TLS group refinement of the ribosome.

tRNA is the elbow, consistent with the fact that this region of tRNA must travel by more than 50 Å during translocation. Interestingly, anisotropic displacement of the elbow is biased in the direction of translocation, orthogonal to the plane of the tRNA (Figures 2(b) and 3(b)).

TLS parameterization of the ribosome represented by 70 rigid groups

The ribosomal subunits contain features that are believed to move independently at different stages of protein synthesis.[26–29] We have performed TLS refinement after splitting the ribosome into 70 rigid groups, represented by ribosomal proteins, tRNAs and rRNA domains (see Materials and Methods). The following discussion concerns TLS analysis of rRNA and tRNA.

Division of the ribosome into 70 groups results in a TLS solution consistent with the ratchet-like mode of intersubunit rotation (REF). Both subunits exhibit dynamic behavior in which their central cores are less mobile than their peripheral parts (Figure 1(d) and (e)). The anisotropic displacement of both subunits is biased toward mutual rotation around the principal axes obtained from the 4-group TLS refinement (previous section), which is especially clear for the small ribosomal RNA (Figure 1(e)). The overall mean displacement of the 23 S rRNA domains is smaller than that of the 16 S rRNA domains (Table 1), suggesting that the large subunit is intrinsically less mobile than the small subunit, consistent with prior observations.[28,30] However, there are two regions of 23 S rRNA that exhibit similar or even higher mobility than the mobile regions of 16 S rRNA. The most mobile region of rRNA is the L1 stalk (Table 1), consistent with cryo-EM[29] and X-ray structures,[21,30–32] which show the L1 stalk in positions that differ by more than 30 Å between different structures. In the ribosome–tRNA complex, where the L1 stalk interacts with the elbow of E-site tRNA, the stalk is oriented toward the middle of the 50 S subunit,[21] while in the vacant ribosome or in the individual large subunit structure the L1 stalk tilts away from the ribosome into solution,[30,31] suggesting that its function is to remove

Table 1. Libration tensor eigenvalues for the 3.7 Å $tRNA^{Phe}$ [20] and 3.8 Å $tRNA^{fMet}$ [21] 70 S ribosome complexes

	Eigenvalues			Eigenvalues	
23 S TLS group	$tRNA^{Phe}$ complex[20]	$tRNA^{fMet}$ complex[21]	16 S TLS group	$tRNA^{Phe}$ complex[20]	$tRNA^{fMet}$ complex[21]
Domain I and h26–35 1–810 and 2895–2902	0.098	0.015	Body 1 (h1–4 and h15–18) 5–51 and 360–562	0.204	0.185
	0.055	0.052		0.194	0.088
	0.000	0.032		0.000	0.010
	0.051[a]	**0.033**		**0.133**	**0.094**
Domain II excluding h26–35 and h42–44 811–990 and 1164–1270	0.128	0.048	Body 2 (h5–14) 52–359	0.065	0.055
	0.085	0.034		0.011	0.040
	0.056	0.067		0.176	0.157
	0.089	**0.05**		**0.084**	**0.084**
L11 stalk (h42–44) 991–1163	0.263	0.122	Platform 1 (h19–20 and h24–27) 563–588 and 756–919	0.307	0.070
	0.512	0.457		0.394	0.172
	0.086	0.058		0.000	0.025
	0.287	**0.212**		**0.234**	**0.089**[b]
	0.236	0.127	Platform 2 (h21–23) 589–755	0.101	0.003
Domain III 1271–1646	0.154	0.050		0.253	0.142
	0.057	0.099		0.000	0.059
	0.149	**0.092**		**0.118**	**0.068**
Domain IV 1647–2010	0.094	0.048	Head 1 (h28–29 and h41–43) 920–949 and 1232–1396	0.334	0.107
	0.030	0.085		0.042	0.000
	0.000	0.000		0.129	0.213
	0.041	**0.044**		**0.168**	**0.107**
Domain V excluding h74–88 2011–2058 and 2448–2627	0.217	0.045	Beak (h30–34) 950–1063 and 1193–1231	0.431	0.178
	0.033	0.000		0.562	0.590
	0.000	0.059		0.000	0.123
	0.083	**0.035**		**0.331**	**0.297**
Domain V excluding h73, h76–78, h89–93 2059–2092 and 2197–2447	0.122	0.000	Head 3 (h35–40) 1064–1192	0.309	0.178
	0.044	0.021		0.019	0.045
	0.025	0.101		0.271	0.395
	0.064	**0.041**		**0.200**	**0.206**
L1 stalk (h76–78) 2093–2196	0.119	0.085	Penultimate stem and 3′ tail (h44–45) 1397–1529	0.000	0.000
	0.373	0.321		0.082	0.051
	0.965	0.863		0.677	0.254
	0.486	**0.423**		**0.253**	**0.102**
	0.121	0.014			
Domain VI 2628–2894	0.067	0.040			
	0.015	0.144			
	0.067	**0.066**			
Average for 23 S	0.146	0.111	Average for 16 S	0.190	0.131

[a] Three libration tensor eigenvalues are shown for each TLS group. The mean eigenvalues are given in **bold**.
[b] The regions of 16 S rRNA that contact the Shine–Dalgarno helix have significantly lower mobilities in the presence of a SD helix, and are indicated by underlined mean libration values.

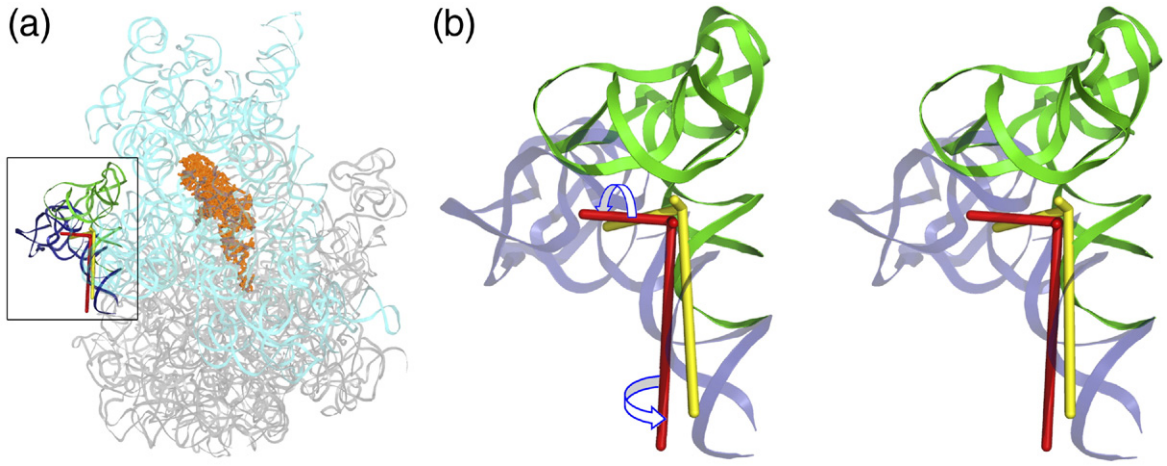

Figure 4. Libration axes for the L1 stalk. (a) Position of the L1 stalk relative to the rest of the ribosome. (b) Stereo view of the location and relative magnitudes of libration axes for the L1 stalk of the $tRNA^{Phe}$ complex (red) and $tRNA^{fMet}$ complex (yellow) are partially consistent with the movement required to displace the L1 stalk of the tRNA-bound complex (green) into the position observed in the vacant ribosome[30] (blue). The relative magnitudes of the libration axes suggest that an additional anisotropic component may arise from a crystal contact involving the L1 stalk.

the deacylated tRNA from the E-site. Location of the libration axes outside of the L1 stalk structure (Figure 4) suggests that its displacement involves significant movement of most of the L1 stalk, consistent with its observed positions.[21,30–32] Rotation around two major libration axes by ~50° with subsequent translation is sufficient to transform the position of the L1 stalk of the tRNA-bound ribosome into that of vacant ribosome (Figure 4). The lengths of the libration axes are not equal, most likely reflecting an additional component of L1 stalk mobility due to contact with the beak of the small subunit of a symmetry-related ribosome.

Another region of 23 S rRNA demonstrating significant mean displacement is the L11 stalk. The L11 stalk interacts with EF-Tu and EF-G[26,33–36] and is therefore implicated in the tRNA-binding and translocation functions. The largest displacement of L11 stalk atoms in the $tRNA^{Phe}$ complex (Figure 5) is in the direction which brings the L11 stalk into the conformation observed in the vacant ribosome, supporting the biological relevance of the dynamics information provided by TLS refinement for this region.

By examining the atomic anisotropic displacements represented by thermal ellipsoids derived from TLS tensors, we have found that the tip of h38 (the "A-site finger") demonstrates anisotropy directed along the axis of α-helix 3 (amino acid residues 68–84) of small-subunit protein S13, with which it

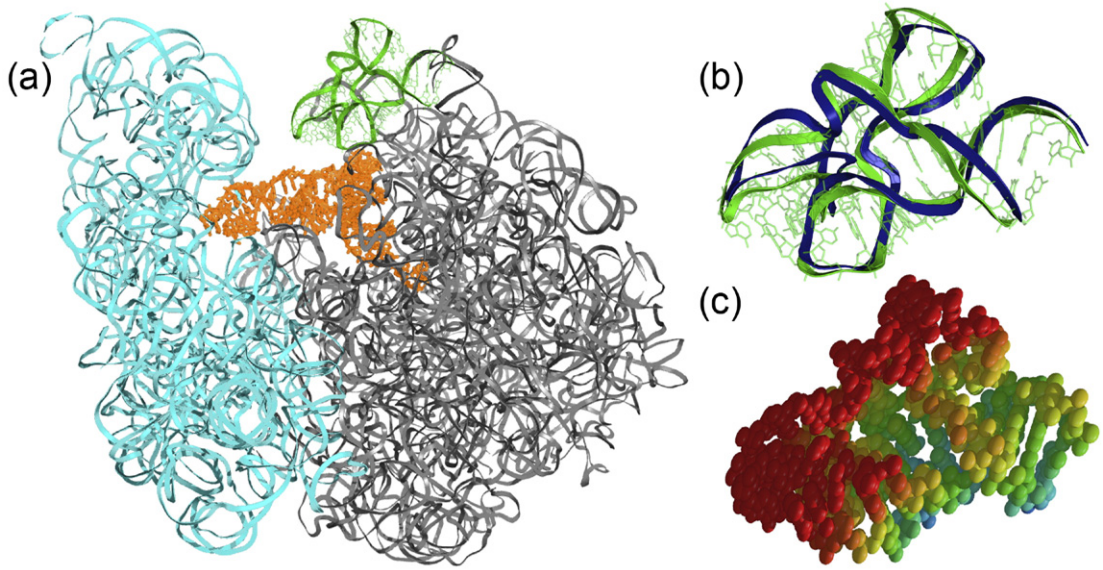

Figure 5. Anisotropic displacement of the L11 stalk derived from the 70-TLS group refinement. (a) Position of L11 stalk relative to the rest of the ribosome. (b) Differences between L11 stalk positions in the $tRNA^{Phe}$ complex (green) and the vacant ribosome[30] (blue) structures when 23 S rRNAs are superimposed. The direction of L11 stalk movement is consistent with anisotropic displacements obtained by TLS refinement. (c) Thermal ellipsoids.

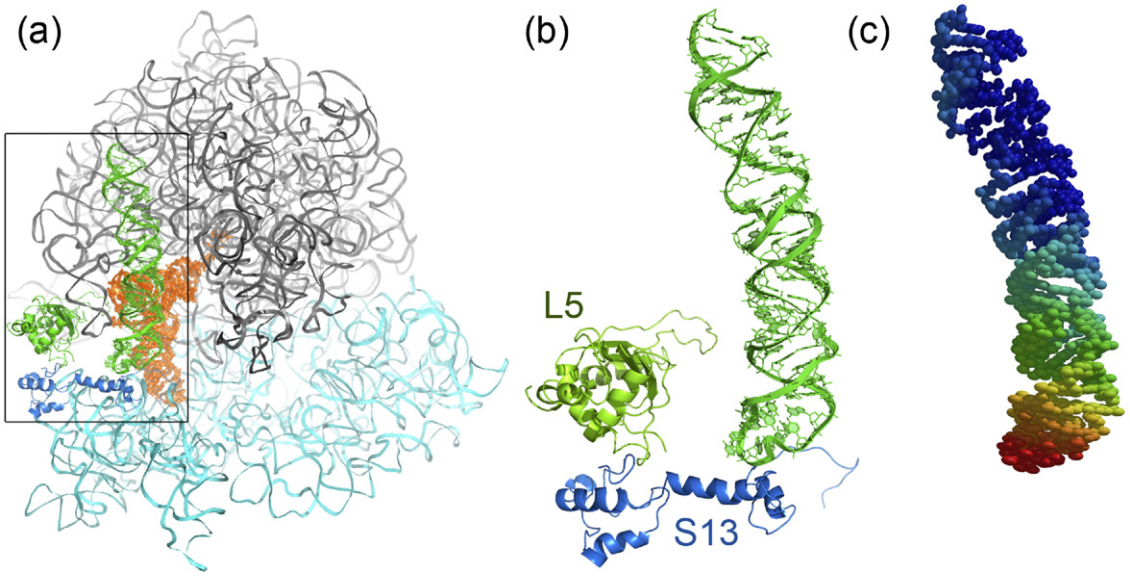

Figure 6. Anisotropic displacement of the A-site finger (h38) derived from the 70-TLS group refinement. (a) Position of the A-site finger relative to the rest of the ribosome. (b) Location of the A-site finger relative to proteins L5 and S13. (c) Thermal ellipsoids showing the bias of anisotropic displacement of the tip of the A-site finger along α-helix 3 of protein S13.

forms intersubunit bridge B1a (Figure 6). Direct comparison of the location of h38 with that in the vacant ribosome is not possible because h38 is disordered in the latter structure. However, ribosomal protein L5, which contacts S13 to form bridge B1b, is displaced anisotropically in the direction of h38 in the $tRNA^{Phe}$ complex.[21,30] Together, these observations suggest that movement of the B1a and B1b bridges may be coupled, although there is no direct interaction between them.

The most mobile part of the small subunit is its so-called beak, at the A-site end of the head (Table 1), whose anisotropic movements may reflect constraints imposed by contact with the L1 stalk of a symmetry-related ribosome. Its different observed orientations may thus be explained, at least in part, by differences in the lattice contacts between ribosomes crystallized in different crystal forms (Figure 7). At the underside of the head, helix 31, whose loop contacts the P-site tRNA anticodon loop *via* m^2G966, is connected by two single-stranded RNA segments to the coaxial helix 30–32 arm. The h31 region shows anisotropic disorder directed between the 30S A and P sites (Figure 8), suggesting that it may be a mobile

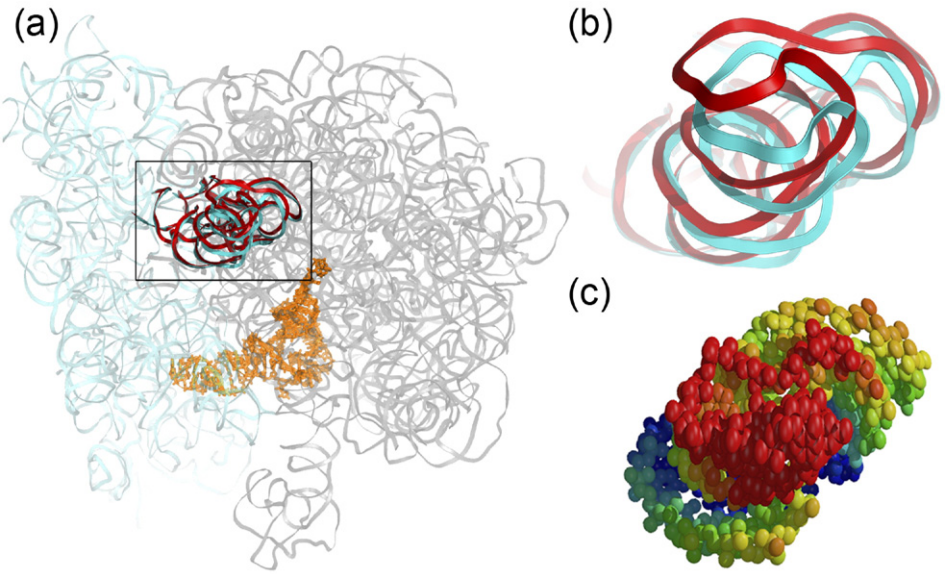

Figure 7. Anisotropic displacement of the tip of the 16 S rRNA beak is likely influenced by crystal contacts. (a) Position of the beak relative to the rest of the ribosome. (b) Superposition of the $tRNA^{Phe}$ complex[21] (cyan) structure with the similar structure of the 2.8 Å $tRNA^{fMet}$ complex crystallized in a different crystal form[25] (red). (c) Thermal ellipsoids derived from the 70-TLS group refinement.

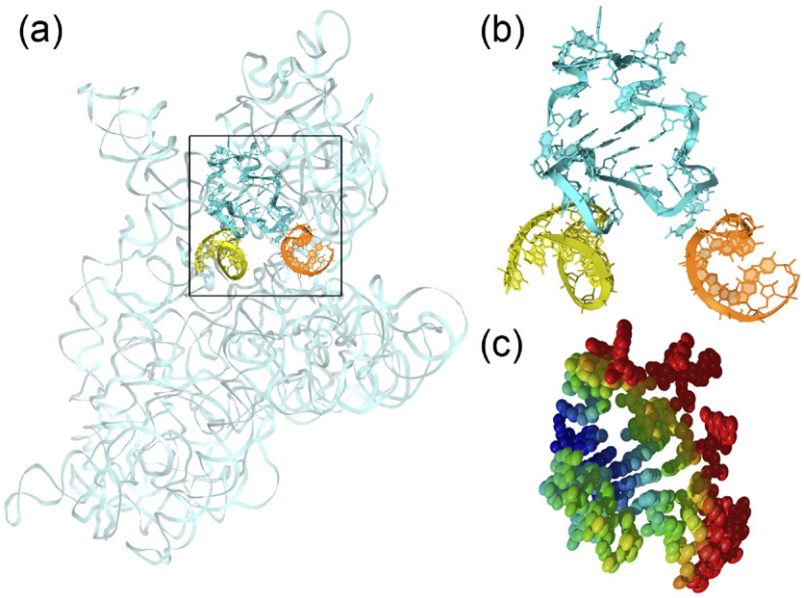

Figure 8. Anisotropic displacements at the base of the 16 S rRNA beak suggest that h31 and its connecting loops may move between the 30 S A and P sites. (a) Position of h31 relative to the rest of 16 S rRNA. (b) Position of h31 (cyan) relative to the anticodon stem loops of the P (orange) and A-site (yellow) tRNAs. (c) Thermal ellipsoids derived from the 70-TLS group refinement.

tRNA-binding element that can follow the movement of tRNA as it translocates from the 30 S A-site to the P-site. The 3′-minor domain of 16 S rRNA comprising h44–45 has a primary libration around an axis oriented almost parallel to the penultimate stem (h44) and located on its inner face. Rotation of the domain around this axis suggests that the outer side of the penultimate stem, which forms several bridges with the large subunit, moves more than the inner side. One of these 50 S subunit contacts, bridge B3, is at or near the axis of intersubunit rotation.[37] This unusual anisotropic movement of h44 may be therefore be related in some way to the mechanics of translocation.

During the 70-group refinement of the ribosome, tRNA molecules were split into their anticodon arm and acceptor arm domains. The relative distribution of atomic anisotropic disorder overall is similar to that derived from refinement with tRNAs treated as single rigid groups (Figures 2 and 3), again placing A26 and G44 among the least mobile nucleotides and the elbow as the most disordered region. Anisotropic displacement of the P-tRNA elbow is biased in the direction of translocation, while the E-tRNA elbow does not show a uniform directional displacement.

Comparison with an independent 3.8 Å X-ray structure of the ribosome

In order to validate the results of TLS refinement of the $tRNA^{Phe}$ complex, TLS parameters were analyzed for an initiation-like 70 S ribosome complex ($tRNA^{fMet}$ complex) determined at 3.8 Å resolution.[22] The $tRNA^{fMet}$ complex contains a $tRNA^{fMet}$ at the P-site and endogenous tRNAs at the E-site and a mRNA with an eight base-pair Shine–Dalgarno sequence. The root-mean-square difference between the phosphate atoms of the ribosomal RNAs for the $tRNA^{Phe}$ and $tRNA^{fMet}$ ribosomes is 0.9 Å.

Eigenvalues of TLS libration tensors for the $tRNA^{Phe}$ and $tRNA^{fMet}$ complexes were strongly correlated for 23 S rRNA and for 16 S rRNA (correlation coefficients = 0.95 and 0.72, respectively). The lower correlation between 16 S rRNAs is likely due to the difference between the mRNAs, as discussed below. In contrast, the eigenvalues for the ribosomal proteins are more weakly correlated (correlation coefficient = 0.30), suggesting that they are not representative of a general functional anisotropy for ribosomal proteins. When determined at resolutions of 3.5 Å and lower, amino acid side-chains of ribosomal proteins are more disordered than rRNA elements, as can be observed in electron density maps[21] or by comparison of *B* factors of known structures solved at similar resolution[21,30]; therefore, TLS formalism may largely reflect coordinate error rather than true functionally related anisotropic displacements of ribosomal proteins. Alternatively, poor TLS parameterization of proteins might be caused by lack of strong restraints (e.g. covalent connections) between protein rigid groups. Since ribosomal RNA accounts for approximately 70% of the mass of the ribosome, and its TLS parameters are strongly correlated between the $tRNA^{Phe}$ and $tRNA^{fMet}$ complex structures, TLS analysis based on ribosomal RNA is more likely to be representative of true anisotropic motions of ribosomal subunits and their sub-domains. This suggestion is also supported by the strong correlation between TLS-predicted movements and structural differences observed for the ribosome stalled in different functional states (Figures 4 and 5).

TLS parameters for the $tRNA^{fMet}$ complex support the conclusion that the large subunit is generally less mobile than the small subunit, with the exception of the L1 and L11 stalks. The L1 stalk and the beak of 16 S rRNA have the highest average mean displacements around their respective librational axes. The greatest discrepancy in mean displacements

between the $tRNA^{Phe}$ and $tRNA^{fMet}$ complexes is for the 30 S subunit neck, platform and 3′-minor domain. Interestingly, all of these regions include features that are constrained by formation of the Shine–Dalgarno (SD) interaction (helix 45 in the 3′ minor domain) or interact with the backbone of the SD helix (the neck and platform). In the $tRNA^{Phe}$ complex, which contains a short mRNA lacking a SD sequence,[21] these sub-domains are signficantly more mobile (average displacement of 0.193) than those in the $tRNA^{fMet}$ complex (average displacement of 0.091), which contains a Shine–Dalgarno helix (Table 1). Thus, the SD helix appears to restrain the mobility of the small subunit sub-domains with which it interacts. This might play a role in optimal positioning of the small subunit for interaction with initiator tRNA during initiation, (for example, promoting optimal interaction between G1338 and A1339 with the minor groove of the anticodon stem[25,38,39]) as was proposed based on comparison of the tRNA-containing ribosome complex with structures of vacant ribosomes and with that representing an elongation-like complex.[30,37]

Analysis of anisotropic motions for the $tRNA^{Phe}$ and $tRNA^{fMet}$ complexes demonstrates that TLS formalism can be applied at lower resolution and to large macromolecular complexes, with some limitations. We have shown that for ribosome structures solved at 3.7–3.8 Å, only ribosomal RNA can be used for interpretation of anisotropic displacements. Therefore, care must be taken when TLS parameters are interpreted at such resolution; it is recommended that TLS results be validated against other biophysical or structural data.

Conclusions

The observed atomic displacements in the 70 S ribosome complex are not random in nature but are directed along pathways that often coincide with the directions of movements that are believed to accompany the processes of protein synthesis. The magnitudes of the TLS librations, however, do not always strictly reflect the functional dynamics of the ribosome, but are sometimes also influenced by constraints dictated by the crystallographic environment. For the most part, the observed anisotropic motions of tRNA molecules, ribosomal subunits and their sub-domains are consistent with large-scale rearrangements that have been detected by X-ray crystallography,[25,30,31,37] cryo-EM[26–29] and other biophysical experiments[2].

Materials and Methods

Starting models and diffraction data

The structures of the 3.7 Å $tRNA^{Phe}$[21] and 3.8 Å $tRNA^{fMet}$[22] from *Thurmus thermophilus* ribosomal complexes containing mRNA, P-and E-tRNAs were downloaded from the Protein Data Bank[40] (PDB accession codes 2OW8 and 1VSA for the former and 2QNH for the latter). Their structures were obtained by real-space[41] and reciprocal-space simulated annealing torsion-angle dynamics and B-group refinement methods[42] as described in Korostelev *et al.*,[21] with the starting models for the structures of ribosomal proteins L15, L19, L21, L28 and L29 adapted from the recent 2.8 Å model of the ribosome.[25] Due to limitations of the 3.7–3.8 Å resolution, grouped isotropic *B*-factors for amino acids and nucleotides, rather than for individual atoms, are available for both models. Structure factor amplitudes, experimental error estimates, and cross-validation information were downloaded from the PDB for the $tRNA^{Phe}$ and $tRNA^{fMet}$ 70 S ribosomal complexes.

TLS refinement procedure

TLS refinement was carried out in REFMAC 5.2[11] and led to reduction in R/R^{free} from 0.365/0.369 ($tRNA^{Phe}$ complex) and 0.342/0362 ($tRNA^{fMet}$ complex) to 0.348/0.359 and 0.324/0.352, respectively. Prior to refinement, all atomic temperature factors were set to a constant value of 60 $Å^2$. A bulk solvent correction model with the parameters of the mask optimized to 1.8 Å (VDWProb), 1.8 Å (IONProb) and 1.1 Å (RSHRink), and overall anisotropic scaling were applied. TLS refinements were carried out using the amplitude-based maximum likelihood function. The refinements converged after three to five cycles; no significant change in R/R^{free} was observed when more than three refinement cycles were carried out. Convergence was also indicatedby the similarities between TLS tensors resulting from refinements carried out for three and ten cycles. Each cycle of TLS refinement was followed by only one to two rounds of positional and *B*-factor refinement with damping factors of 0.25 (for positional and *B*-factor shifts at each step) in order to minimize overfitting.

Choice of the number of TLS groups

Each TLS group contributes 20 refinement parameters; therefore, using up to 100 TLS groups does not significantly increase the total number of refinement parameters for the ribosome, which has nearly 150,000 atoms. We have tested TLS refinements using 4, 70 and 100 TLS groups. Since ribosomes consist of two subunits, which have been shown to move with respect to each other during translocation,[1–3] the two subunits and the two tRNAs bound to the P and E sites were treated as individual rigid bodies in 4-group TLS refinements. The rationale for using 70 TLS groups comes from the observation that ribosomal proteins, sub-domains of ribosomal RNA and of tRNAs can move with respect to each other at different stages of protein synthesis.[26,28] Thus, the next "crude" division of the ribosome involved treating each of the ribosomal proteins (47 proteins are modeled in each of the 70 S complexes used), 5 S rRNA, nine sub-domains of 23 S rRNA (Table 1), eight sub-domains of 16S rRNA (Table 1), anticodon arm (nucleotides 8–48) and acceptor arm (nucleotides 1–7 and 49–76) domains of tRNAs (for both P and E-site tRNAs) as individual TLS groups. The designation of the boundaries of different groups within the ribosomal RNAs was based on our knowledge of the domain structure of the rRNA. The regions connecting well-defined sub-domains were chosen as boundaries and did not include secondary structure elements such as helices and loops. mRNA was not included in the TLS refinement of the $tRNA^{Phe}$

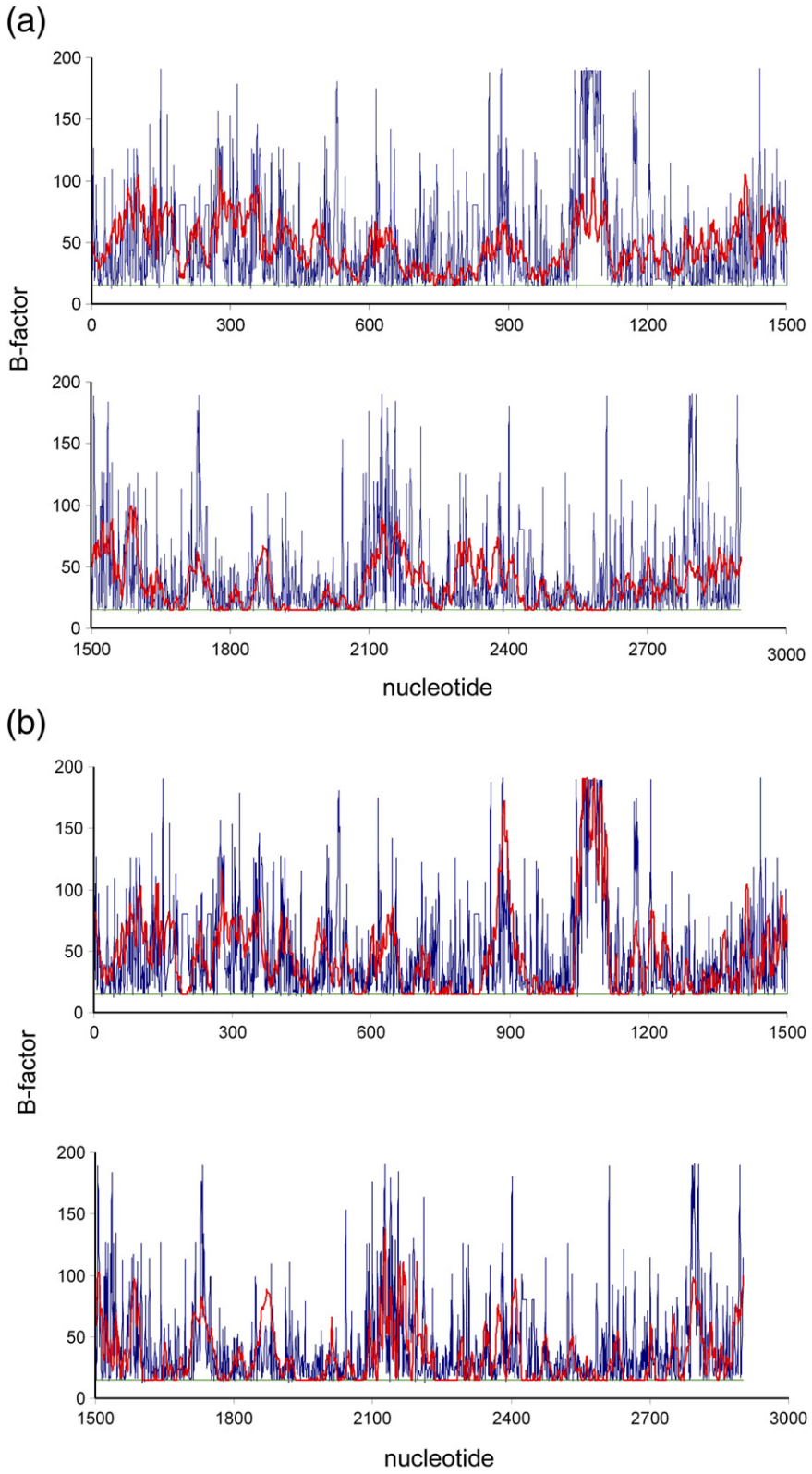

Figure 9. Modeling of isotropic *B* factors by TLS refinement. Residue-averaged TLS-derived *B* factors (B_{iso}, red) and grouped *B* factors of the initial 70 S ribosome model (B_{group}, blue) are plotted *versus* corresponding nucleotides of the 23 S ribosomal RNA. B_{iso} factors resulting from the 4-group refinement (a) are less well correlated with the B_{group} factors from the initial model than those resulting from the 70-group refinement (b) (correlation coefficients are 0.33 and 0.5, respectively). The residual *B* factor after TLS refinement (green) is low and essentially constant, which reflects the stability of the TLS refinements.

complex since only six nucleotides of mRNA are modeled. In the $tRNA^{fMet}$ 70 S complex, the 5′ region of the modeled 18 nucleotide mRNA forms the Shine–Dalgarno helix with the 3′ tail of the small subunit rRNA and therefore the mRNA was combined with the 3′-terminal nucleotides (1534–1541) of 16 S rRNA into one group. Overall, 69 TLS groups were used for the $tRNA^{Phe}$ complex and 70 groups for the $tRNA^{fMet}$ complex; for simplicity, both refinements are referred to as 70-group refinements. During the 100-group TLS refinement, 16 S and 23 S rRNAs were split into finer pieces comprised of secondary structure elements.

Refinement of 70 TLS groups yielded R/R^{free} values that were marginally lower than those obtained by refinement of 4 TLS groups (0.3478/0.359 *versus* 0.3486/0.3599), while TLS refinement with 100 TLS domains was unstable and led to negative eigenvalues for librational tensors. Similar crystallographic residuals for the 4 and 70-domain TLS refinements might suggest that modeling the ribosome as four TLS regions is sufficient to infer most of the ribosome dynamics information that TLS refinement can provide. In order to test this hypothesis, we have analyzed the TLS-derived temperature factors for 23 S rRNA, which is the largest constituent of the ribosome. The 23 S rRNA was treated as a single TLS group (combined with 5 S rRNA and large-subunit proteins) during the 4-group refinement and was split into nine sub-domains (Table 1) in the 70-group refinement. Isotropic *B* factors were calculated as the traces of the corresponding atomic anisotropic temperature factors derived from decomposition of the TLS tensors.[43] These isotropic *B* factors (B_{iso}) were averaged for each residue of 23 S rRNA and then compared to the original grouped *B*-factors (B_{group}), which range between 15 and 200. Since the residual (B_{res}) resulting from TLS refinement refined to values lower than 15 (as low as 3 for the-group refinement and 1 for the 70-group refinement), a scaling factor was applied to B_{res} and B_{iso} so that B_{iso} values range between 15 and 200 and thus are on the same scale as B_{group}. Comparison of the isotropic *B*-factors with grouped *B*-factors revealed that the 70-group TLS refinement leads to a significantly better description of the temperature factors than the 4-group refinement (Figure 9): the correlation coefficient for the residue-averaged B_{iso} with B_{group} for the whole 23 S rRNA (2902 nucleotides) is 1.5 times higher for the 70-group refinement than that for the 4-group refinement (0.5 *versus* 0.33). This suggests that while there is only marginal improvement in R/R_{free} upon splitting of the ribosome into finer TLS groups, the 70-group TLS analysis provides a more detailed characterization of the structural dynamics of the ribosome.

Parameterization of 70 TLS groups for the $tRNA^{Phe}$ and $tRNA^{fMet}$ 70 S ribosome structures leads to the following results. Unlike libration, the translational and screw tensors have eigenvalues that are approximately equal in all directions and small in absolute value for the different rigid groups, yielding average mean-square displacements of less than 0.008 A^2 (translation) and 0.007 A*degree (screw) for the whole ribosome. The average mean-square displacement around librational axes is 0.51 $degree^2$, indicating that librational motion has the most significant contribution to anisotropic disorder of the ribosomal rigid groups. Eigenvalues of the librational tensors are positive for all TLS groups, showing that TLS refinement was stable and that assignment of rigid groups is physically reasonable.

Atomic anisotropic displacement parameters were calculated by using TLSANL[43] by decomposition of the TLS tensors. TLSANL was also employed to generate axes and to calculate eigenvalues for tensors representing translational, librational and screw motions. PyMOL[44] and Rastep[45] were used for visualization of atomic models, TLS axes and atomic thermal ellipsoids. Coordinates for librational axes of ribosomal RNA regions presented in Table 1 can be downloaded in PDB format†.

Acknowledgements

This work was supported by grants no. GM-17129 and GM-59140 (to H.F.N.) from the NIH. We thank Sergei Trakhanov and Martin Laurberg for their contributions to structure determination.

References

1. Frank, J. & Agrawal, R. K. (2000). A ratchet-like intersubunit reorganization of the ribosome during translocation. *Nature*, **406**, 318–322.
2. Ermolenko, D. N., Majumdar, Z. K., Hickerson, R. P., Spiegel, P. C., Clegg, R. M. & Noller, H. F. (2007). Observation of intersubunit movement of the ribosome in solution using FRET. *J. Mol. Biol.* **370**, 530–540.
3. Horan, L. H. & Noller, H. F. (2007). Intersubunit movement is required for ribosomal translocation. *Proc. Natl. Acad. Sci. USA*, **104**, 4881–4885.
4. Pestka, S. (1969). Studies on the formation of transfer ribonucleic acid-ribosome complexes. VI. Oligopeptide synthesis and translocation on ribosomes in the presence and absence of soluble transfer factors. *J. Biol. Chem.* **244**, 1533–1539.
5. Gavrilova, L. P. & Spirin, A. S. (1971). Stimulation of "non-enzymic" translocation in ribosomes by p-chloromercuribenzoate. *FEBS Letters*, **17**, 324–326.
6. Gavrilova, L. P., Kostiashkina, O. E., Koteliansky, V. E., Rutkevitch, N. M. & Spirin, A. S. (1976). Factor-free ("non-enzymic") and factor-dependent systems of translation of polyuridylic acid by Escherichia coli ribosomes. *J. Mol. Biol.* **101**, 537–552.
7. Southworth, D. R., Brunelle, J. L. & Green, R. (2002). EFG-independent translocation of the mRNA:tRNA complex is promoted by modification of the ribosome with thiol-specific reagents. *J. Mol. Biol.* **324**, 611–623.
8. Fredrick, K. & Noller, H. F. (2003). Catalysis of ribosomal translocation by sparsomycin. *Science*, **300**, 1159–1162.
9. Cruickshank, D. W. J. (1956). The determination of the anisotropic thermal motion of atoms in crystals. *Acta Crystallog.* **9**, 747–753.
10. Dunitz, J. D., Schomaker, V. & Trueblood, K. N. (1988). Interpretation of atomic displacement parameters from diffraction studies of crystals. *J. Phys. Chem.* **92**, 856–867.
11. Winn, M. D., Murshudov, G. N. & Papiz, M. Z. (2003). Macromolecular TLS refinement in REFMAC

†http://rna.ucsc.edu/rnacenter/pdb/TLS_axes_rRNA_3.7A.pdb

at moderate resolutions. *Methods Enzymol.* **374**, 300–321.
12. Harata, K., Abe, Y. & Muraki, M. (1999). Crystallographic evaluation of internal motion of human alpha-lactalbumin refined by full-matrix least-squares method. *J. Mol. Biol.* **287**, 347–358.
13. Wilson, M. A. & Brunger, A. T. (2000). The 1.0 Å crystal structure of Ca(2+)-bound calmodulin: an analysis of disorder and implications for functionally relevant plasticity. *J. Mol. Biol.* **301**, 1237–1256.
14. Diamond, R. (1990). On the use of normal modes in thermal parameter refinement: theory and application to the bovine pancreatic trypsin inhibitor. *Acta Crystallog. sect. A*, **46**, 425–435.
15. Kidera, A. & Go, N. (1992). Normal mode refinement: crystallographic refinement of protein dynamic structure. I. Theory and test by simulated diffraction data. *J. Mol. Biol.* **225**, 457–475.
16. Yousef, M. S., Clark, S. A., Pruett, P. K., Somasundaram, T., Ellington, W. R. & Chapman, M. S. (2003). Induced fit in guanidino kinases–comparison of substrate-free and transition state analog structures of arginine kinase. *Protein Sci.* **12**, 103–111.
17. Chaudhry, C., Horwich, A. L., Brunger, A. T. & Adams, P. D. (2004). Exploring the structural dynamics of the *E.coli* chaperonin GroEL using translation-libration-screw crystallographic refinement of intermediate states. *J. Mol. Biol.* **342**, 229–245.
18. Schomaker, V. & Trueblood, K. N. (1968). On the rigid-body motion of molecules in crystals. *Acta Crystallog. sect. B*, **24**, 63–76.
19. Schomaker, V. & Trueblood, K. N. (1998). Correlation of internal torsional motion with overall molecular motion in crystals. *Acta Crystallog. sect. B*, **54**, 507–514.
20. Howlin, B., Moss, D. S. & Harris, G. W. (1989). Segmented anisotropic refinement of bovine ribonuclease A by the application of the rigid-body TLS model. *Acta Crystallog. sect. A*, **45**, 851–861.
21. Korostelev, A., Trakhanov, S., Laurberg, M. & Noller, H. F. (2006). Crystal structure of a 70S ribosome-tRNA complex reveals functional interactions and rearrangements. *Cell*, **126**, 1065–1077.
22. Korostelev, A., Trakhanov, S., Asahara, H., Laurberg, M. & Noller, H. F. (2007). Interactions and Dynamics of the Shine-Dalgarno Helix in the 70S Ribosome. *Proc. Natl. Acad. Sci. USA*. In the press.
23. Ogle, J. M., Brodersen, D. E., Clemons, W. M., Tarry, M. J., Carter, A. P. & Ramakrishnan, V. (2001). Recognition of cognate transfer RNA by the 30S ribosomal subunit. *Science*, **292**, 897–902.
24. Schmeing, T. M., Huang, K. S., Strobel, S. A. & Steitz, T. A. (2005). An induced-fit mechanism to promote peptide bond formation and exclude hydrolysis of peptidyl-tRNA. *Nature*, **438**, 520–524.
25. Selmer, M., Dunham, C. M., Murphy, F. V. t., Weixlbaumer, A., Petry, S., Kelley, A. C. *et al.* (2006). Structure of the 70S ribosome complexed with mRNA and tRNA. *Science*, **313**, 1935–1942.
26. Valle, M., Zavialov, A., Li, W., Stagg, S. M., Sengupta, J., Nielsen, R. C. *et al.* (2003). Incorporation of aminoacyl-tRNA into the ribosome as seen by cryo-electron microscopy. *Nature Struct. Biol.* **10**, 899–906.
27. Valle, M., Zavialov, A., Sengupta, J., Rawat, U., Ehrenberg, M. & Frank, J. (2003). Locking and unlocking of ribosomal motions. *Cell*, **114**, 123–134.
28. Gao, H., Sengupta, J., Valle, M., Korostelev, A., Eswar, N., Stagg, S. M. *et al.* (2003). Study of the structural dynamics of the *E coli* 70S ribosome using real-space refinement. *Cell*, **113**, 789–801.
29. Tama, F., Valle, M., Frank, J. & Brooks, C. L., 3rd (2003). Dynamic reorganization of the functionally active ribosome explored by normal mode analysis and cryo-electron microscopy. *Proc. Natl. Acad. Sci. USA*, **100**, 9319–9323.
30. Schuwirth, B. S., Borovinskaya, M. A., Hau, C. W., Zhang, W., Vila-Sanjurjo, A., Holton, J. M. & Cate, J. H. (2005). Structures of the bacterial ribosome at 3.5 Å resolution. *Science*, **310**, 827–834.
31. Harms, J., Schluenzen, F., Zarivach, R., Bashan, A., Gat, S., Agmon, I. *et al.* (2001). High resolution structure of the large ribosomal subunit from a mesophilic eubacterium. *Cell*, **107**, 679–688.
32. Ban, N., Nissen, P., Hansen, J., Moore, P. B. & Steitz, T. A. (2000). The complete atomic structure of the large ribosomal subunit at 2.4 Å resolution. *Science*, **289**, 905–920.
33. Moazed, D., Robertson, J. M. & Noller, H. F. (1988). Interaction of elongation factors EF-G and EF-Tu with a conserved loop in 23S RNA. *Nature*, **334**, 362–364.
34. Agrawal, R. K., Heagle, A. B., Penczek, P., Grassucci, R. A. & Frank, J. (1999). EF-G-dependent GTP hydrolysis induces translocation accompanied by large conformational changes in the 70S ribosome. *Nature Struct. Biol.* **6**, 643–647.
35. Agrawal, R. K., Penczek, P., Grassucci, R. A. & Frank, J. (1998). Visualization of elongation factor G on the *Escherichia coli* 70S ribosome: the mechanism of translocation. *Proc. Natl. Acad. Sci. USA*, **95**, 6134–6138.
36. Stark, H., Rodnina, M. V., Wieden, H. J., van Heel, M. & Wintermeyer, W. (2000). Large-scale movement of elongation factor G and extensive conformational change of the ribosome during translocation. *Cell*, **100**, 301–309.
37. Yusupov, M., Yusupova, G., Baucom, A., Lieberman, K., Earnest, T. N., Cate, J. H. & Noller, H. F. (2001). Crystal structure of the ribosome at 5.5 Å resolution. *Science*, **292**, 883–896.
38. Dallas, A. & Noller, H. F. (2001). Interaction of translation initiation factor 3 with the 30S ribosomal subunit. *Mol. Cell*, **8**, 855–864.
39. Lancaster, L. & Noller, H. F. (2005). Involvement of 16S rRNA nucleotides G1338 and A1339 in discrimination of initiator tRNA. *Mol. Cell*, **20**, 623–632.
40. Berman, H. M., Battistuz, T., Bhat, T. N., Bluhm, W. F., Bourne, P. E., Burkhardt, K. *et al.* (2002). The Protein Data Bank. *Acta Crystallog. sect. D*, **58**, 899–907.
41. Korostelev, A., Bertram, R. & Chapman, M. S. (2002). Simulated-annealing real-space refinement as a tool in model building. *Acta Crystallog. sect. D*, **58**, 761–767.
42. Brünger, A. T., Adams, P. D., Clore, G. M., DeLano, W. L., Gros, P., Grosse-Kunstleve, R. W. *et al.* (1998). Crystallography and NMR system: a new software suite for macromolecular structure determination. *Acta Crystallog. sect. D*, **54**, 905–921.
43. Howlin, B., Butler, S. A., Moss, D. S., Harris, G. W. & Driessen, H. P. C. (1993). TLSANL: TLS parameter-analysis program for segmented anisotropic refinement of macromolecular structures. *J. Appl. Crystallog.* **26**, 622–624.
44. DeLano, W. L. (2002). *The PyMOL Molecuar Graphics System User's Manual*, DeLano Scientific, Palo Alto, CA.
45. Merritt, E. A. & Murphy, M. E. P. (1994). Raster3D version 2.0: a program for photorealistic molecular graphics. *Acta Crystallog. sect. D*, **50**, 869–873.